International Conference on Mathematics, Computational Methods & Reactor Physics (M&C 2009)
Saratoga Springs, New York, May 3-7, 2009, on CD-ROM, American Nuclear Society, LaGrange Park, IL (2009)

LEVERMORE-POMRANING MODEL RESULTS FOR AN INTERIOR SOURCE BINARY STOCHASTIC MEDIUM BENCHMARK PROBLEM

Patrick S. Brantley
Lawrence Livermore National Laboratory
P.O. Box 808, L-023
Livermore, CA 94551 USA
brantley1@llnl.gov

Todd S. Palmer
Department of Nuclear Engineering and Radiation Health Physics
Oregon State University
116 Radiation Center
Corvallis, OR 97331-5902 USA
palmerts@engr.orst.edu

ABSTRACT

The accuracy of the Levermore-Pomraning model for particle transport through a binary stochastic medium is investigated using an interior source benchmark problem. As in previous comparisons of the model for incident angular flux benchmark problems, the model accurately computes the leakage and the scalar flux distributions for optically thin slabs. The model is less accurate for more optically thick slabs but has a maximum relative error in the leakage of approximately 10% for the problems examined. The maximum root-mean-squared relative errors for the total and material scalar flux distributions approach 65% for the more optically thick slabs. Consistent with previous benchmark comparisons, the results of these interior source benchmark comparisons demonstrate that the Levermore-Pomraning model produces qualitatively correct and semi-quantitatively correct results for both leakage values and scalar flux distributions.

Key Words: particle transport benchmark, binary stochastic mixture, Levermore-Pomraning model

1. INTRODUCTION

Particle transport through binary stochastic mixtures has received considerable research attention in the last two decades [1, 2]. Much of the research has focused on the development and analysis of approximate deterministic models for the solution of such particle transport problems. The most ubiquitous approximate deterministic model is often referred to as the Levermore-Pomraning or the Standard Model [2]. The accuracy of the Levermore-Pomraning model has previously been examined by Adams et al. [3] using a set of benchmark problems involving a non-stochastic isotropic angular flux incident on one boundary of a one-dimensional planar geometry binary stochastic medium. The benchmark suite is characterized by nine different sets of material cross sections, mean material slab widths, and material scattering ratios as well as three different total slab widths. The material statistics are assumed to be Markovian and spatially homogeneous. The fiducial quantities for comparison are the ensemble-averaged reflection and transmission through the slab. Zuchuat et al. [4] extended these planar geometry

benchmark solutions and Levermore-Pomraning model comparisons to include the ensemble-averaged total and material scalar flux distributions.

In this paper, we investigate the accuracy of the Levermore-Pomraning model for a related set of one-dimensional planar geometry interior source benchmark problems. To our knowledge, a systematic study of the accuracy of the planar geometry Levermore-Pomraning model for a problem driven by an interior source has never been published (although an isolated interior source result was recently published by Sanchez [5].) Because the interior source scalar flux distributions are of an inherently different character than the distributions obtained for the incident angular flux benchmark problems, this benchmark comparison extends the domain of problems for which the accuracy of the Levermore-Pomraning model has been investigated. The material specifications of the binary stochastic medium examined in this paper are the same as for the standard set of benchmark problems first examined by Adams et al. [3], but the benchmark problems are driven by a uniform isotropic interior source rather than an isotropic incident angular flux. The benchmark solutions to these problems were obtained using the Monte Carlo procedure described in [3] in which independent material realizations are sampled from the Markovian statistics and the transport problem is solved for each realization using the discrete ordinates transport method [6]. 5×10^5 independent realizations were simulated and the results averaged to obtain ensemble-averaged values for the leakage from the slab. We also tabulate the ensemble-averaged total and material scalar flux distributions using the procedure described in Ref. [4].

The Levermore-Pomraning model solutions in this paper were obtained using the discrete ordinates angular approximation and the simple corner balance spatial discretization [7]. The iterative solution uses a diffusion synthetic acceleration algorithm to accelerate convergence [8].

The remainder of this paper is organized as follows. In Section 2, we describe the interior source benchmark transport problem we use to assess the accuracy of the Levermore-Pomraning model. We also describe the process used to obtain the benchmark solutions. We briefly describe the Levermore-Pomraning model in Section 3. We present numerical comparisons of the Levermore-Pomraning model solutions to the benchmark solutions in Section 4. We give general conclusions and possible directions for future work in Section 5.

2. BENCHMARK TRANSPORT PROBLEMS

We consider the following time-independent monoenergetic neutron transport problem with isotropic scattering in a one-dimensional planar geometry spatial domain defined on $0 \leq x \leq L$:

$$\mu \frac{\partial}{\partial x} \psi(x,\mu) + \sigma_t(x)\,\psi(x,\mu) = \frac{1}{2}\sigma_s(x) \int_{-1}^{1} \psi(x,\mu')\,d\mu' + \frac{1}{2} q(x) \quad ,$$

$$0 \leq x \leq L \ , \ -1 \leq \mu \leq 1 \ , \tag{1}$$

$$q(x) = \frac{1}{L} \ , \ 0 \leq x \leq L \ , \tag{2}$$

$$\psi(0,\mu) = 0 \ , \ \mu > 0 \ , \tag{3}$$

$$\psi\left(L,\mu\right)=0\ \ ,\ \ \mu<0\ \ . \tag{4}$$

Eqs. (1)–(4) are written in standard neutronics notation [6]. The interior source defined by Eq. (2) is non-stochastic, spatially uniform, and results in one neutron sourced into the medium per unit time. The vacuum boundary conditions given by Eqs. (3) and (4) are non-stochastic. The stochastic spatial medium is assumed to be composed of alternating slabs of two materials, labelled with the indices 0 and 1, with the mean material slab width for material i denoted as Λ_i. The total and scattering cross sections for each material are uniform and are denoted as σ_t^i and σ_s^i, $i=0,1$, respectively. The distribution of material slab widths in the planar medium is assumed to be described by spatially homogeneous Markovian statistics [2], in which case a slab width for material i, λ_i, can be sampled from an exponential distribution given by

$$f_i\left(\lambda_i\right)=\frac{1}{\Lambda_i}\exp\left(-\frac{\lambda_i}{\Lambda_i}\right)\ \ . \tag{5}$$

Given the mean material slab widths, the probability of finding material i at any given point in the spatial domain, p_i, is given by

$$p_i=\frac{\Lambda_i}{\Lambda_0+\Lambda_1}\ \ . \tag{6}$$

This material probability corresponds to the volume fraction of the material in the problem.

The fiducial comparison quantities are the ensemble-averaged leakage from the slab at $x=0$, $\langle J_0\rangle$, defined as

$$\langle J_0\rangle=\int_{-1}^{0}|\mu|\left\langle\psi\left(0,\mu\right)\right\rangle d\mu\ \ , \tag{7}$$

and the ensemble-averaged leakage from the slab at $x=L$, $\langle J_L\rangle$, defined as

$$\langle J_L\rangle=\int_{0}^{1}\mu\left\langle\psi\left(L,\mu\right)\right\rangle d\mu\ \ . \tag{8}$$

In the limit of an infinite number of realizations, the leakage at the left and right boundaries of the slab should be identical, i.e. $\langle J_0\rangle=\langle J_L\rangle$. Given the finite number of realizations used in the generation of our benchmark results, we choose to simply compare the leakage from the slab at $x=L$, $\langle J_L\rangle$. In addition, we compare the ensemble-averaged total and material scalar flux distributions, $\langle\phi\left(x\right)\rangle$ and $\langle\phi_i\left(x\right)\rangle$, $i=0,1$, respectively, as these distributions determine reaction rates in the system.

The material parameters for the benchmark transport problems are given in Table I using the notation of Ref. [4]. The scattering ratio for material i is defined as $c_i=\sigma_s^i/\sigma_t^i$. For each set of material parameters (cases 1, 2, and 3), three sets of scattering ratio combinations (cases a, b, and c) and three slab widths (L = 0.1, 1.0, and 10.0) are considered. For all cases, the ensemble-averaged total cross section, defined as $\langle\sigma_t\rangle=p_0\sigma_t^0+p_1\sigma_t^1$, is unity. The different case numbers (i.e. 1, 2, and 3) represent permutations of materials with mean materal slab widths of optical depth 0.1, 1.0, and 10.0. The different case letters (i.e. a, b, and c) represent varying amounts of scattering for each material.

We generated the benchmark solutions, including scalar flux distributions, using the methodologies described in Refs. [3] and [4]. We now briefly describe this benchmark procedure.

Table I. Material parameters for benchmark transport problems

Case	σ_t^0	Λ_0	σ_t^1	Λ_1	Case	c_0	c_1	L
1	10/99	99/100	100/11	11/100	a	0.0	1.0	0.1
2	10/99	99/10	100/11	11/10	b	1.0	0.0	1.0
3	2/101	101/20	200/101	101/20	c	0.9	0.9	10.0

One instance of the material realization is generated by first sampling the material located at $x = 0$ using the probabilities defined in Eq. (6). Given this sampled material, a material slab width is sampled from the Markovian exponential distribution, Eq. (5), using the mean material slab width, Λ_0 or Λ_1, corresponding to the sampled material. The material slab width for the next (different) material is then sampled in the same manner. This process is repeated until the sum of the sampled material slab widths equals the total slab width L. The last sampled material slab width may require truncation to the total slab width. Given this single material realization, the transport problem described by Eqs. (1)–(4) is then solved for that realization using a discrete ordinates transport code. This procedure is repeated a large number M of times and the results averaged to obtain ensemble-averaged values. The ensemble-averaged leakage at $x = L$ is computed as [3]

$$\langle J_L \rangle = \frac{1}{M} \sum_{m=1}^{M} \int_0^1 \mu \psi_m (L, \mu) \, d\mu \quad , \tag{9}$$

where $\psi_m (L, \mu)$ is the angular flux at $x = L$ computed for realization m, and the angular integral is performed using the same quadrature as in the discrete ordinates calculation. An analogous expression holds for the leakage at $x = 0$. The ensemble-averaged total scalar flux distribution is computed as [4]

$$\langle \phi (x) \rangle = \frac{1}{M} \sum_{m=1}^{M} \phi_m (x) \quad , \tag{10}$$

where $\phi_m (x)$ is the total scalar flux distribution for realization m at spatial location x. The computation of the ensemble-averaged material scalar flux distributions is slightly more complicated. The ensemble-averaged material i scalar flux distribution is computed as [4]

$$\langle \phi_i (x) \rangle = \frac{1}{M_i} \sum_{m_i=1}^{M_i} \phi_{m_i} (x) \quad , \tag{11}$$

where $M_i \leq M$ is the number of realizations with material i present at location x, and the sum is computed only for those realizations.

The discrete ordinates transport code used to generate the benchmark solutions utilizes the linear discontinuous spatial discretization with the mesh spacing in each material chosen such that $\frac{\sigma_t^i \Delta x}{|\mu|_{min}} \leq \frac{1}{10}$, where $|\mu|_{min}$ is the minimum cosine in the quadrature set [6]. 5×10^5 independent statistical material realizations were sampled from Markovian statistics and simulated for each case. The total and material scalar flux distributions were tallied at the edges of 100 uniformly-spaced spatial zones. (We enforced a minimum of 100 spatial zones for each independent material realization.)

We found that angular convergence for the optically thin slabs (i.e. $L = 0.1$) could only be achieved using very high quadrature orders for these interior source benchmark problems. This convergence difficulty is not entirely unexpected, as optically thin problems are known to require high order quadrature sets to converge because of the effect of the vacuum boundaries [6]. We examined in detail the case 1a benchmark problem for $L = 0.1$. This particular case has one highly probable material, material zero with $p_0 = 0.9$, with a small total cross section, $\sigma_t^0 = 10/99$, resulting in many realizations being composed of optically thin slabs of width $\sigma_t^0 \Delta x = 1/99$ mean free paths. The solution of this problem was not converged in angle using a standard S_{96} Gauss-Legendre quadrature set. This same problem was converged in angle when using a S_{96} double-P_N quadrature set [6]. Based on this result, we used a double-P_N quadrature set with $N = 96$ for the problems with total slab widths of $L = 0.1$ and 1.0 and a standard Gauss-Legendre quadrature set with $N = 64$ for the problems with a total slab width of $L = 10.0$.

We computed the transport solution for each material realization using an unmodified planar geometry discrete ordinates transport code written in Fortran. We performed the calculation of the ensemble-averaged results using a Python language driver script (less than 400 lines of actual code) that 1) samples each material realization, 2) generates and writes to disk an input file for the discrete ordinates transport code corresponding to the sampled material realization, 3) runs the transport code, 4) parses standard output files from the transport code to obtain the computed leakage values and scalar flux distributions for that material realization, 5) computes the required ensemble-averaged sums over all material realizations, and 6) writes the ensemble-averaged results to a summary file. As the generation of these benchmark solutions is a process to be performed only a limited number of times, this approach has the significant advantage of requiring no modification or specialization (and associated testing) of the discrete ordinates transport code for the solution of these benchmark problems. An obvious disadvantage to this approach is that the linkage of the Python processing script to the transport code via writing input files and parsing output files possesses an inherent inefficiency. To ameliorate this inefficiency, we utilized the pyMPI [9] Python extension to parallelize using the MPI message passing interface [10] the sampling of the independent material realizations and the solution of the transport problems for each of these realizations. This parallelization is very efficient, as each MPI process can independently sample a subset of the total number of material realizations and solve the corresponding transport problems with no parallel communication with other processes required until all of its computational work is completed. Care must be exercised to ensure that independent random number streams are utilized on each MPI process. The benchmark solutions described in this paper were obtained using typically 512 processors of a Linux cluster with sixteen AMD Opteron 2.3 GHz processors per compute node. Each benchmark case required a few to several hours of simulation time.

Using the same procedure and coding, we have regenerated the benchmark solutions to the standard set of benchmark problems defined in Ref. [3]. We compared our benchmark solutions against the probabilities of reflection and transmission published in Refs. [3] and [4], finding agreement to typically two to three digits, and against the scalar flux distribution data remaining available [11] from Ref. [4]. These comparisons establish confidence that our benchmark procedure is consistent with previously published benchmark results.

3. LEVERMORE-POMRANING MODEL

The Levermore-Pomraning model approximation to Eqs. (1)–(4), assuming spatially homogeneous and time-independent statistics, is given by [1, 2]:

$$\mu\frac{\partial}{\partial x}\psi_i\left(x,\mu\right)+\sigma_t^i\psi_i\left(x,\mu\right)=\frac{1}{2}\sigma_s^i\int_{-1}^{1}\psi_i\left(x,\mu'\right)d\mu'+\frac{|\mu|}{\Lambda_i}\left[\psi_j\left(x,\mu\right)-\psi_i\left(x,\mu\right)\right]+\frac{1}{2}q_i\left(x\right)\ \ ,$$

$$0\leq x\leq L\ \ ,\ \ -1\leq\mu\leq 1\ \ , \tag{12}$$

$$q_i\left(x\right)=\frac{1}{L}\ \ ,\ \ 0\leq x\leq L\ \ , \tag{13}$$

$$\psi_i\left(0,\mu\right)=0\ \ ,\ \ \mu>0\ \ , \tag{14}$$

$$\psi_i\left(L,\mu\right)=0\ \ ,\ \ \mu<0\ \ , \tag{15}$$

for the material index $i=0,1$ and $j\neq i$. Here $\psi_i\left(x,\mu\right)$ is the material i angular flux at spatial location x in direction μ. The numerical solutions to Eqs. (12)–(15) presented in this paper were obtained using the standard discrete ordinates angular approximation and the simple corner balance spatial discretization [7] with 100,000 uniformly-spaced spatial zones. These simulations used an S_{128} double-P_N quadrature set for the $L=0.1$ and $L=1.0$ slabs and an S_{128} standard Gauss-Legendre quadrature set for the $L=10.0$ slab. The iterative solution uses a diffusion synthetic acceleration algorithm to accelerate convergence [8] and required in all cases eleven or less iterations to converge to a tolerance of 10^{-8}.

4. NUMERICAL COMPARISONS TO BENCHMARK PROBLEMS

In this section, we evaluate the accuracy of the Levermore-Pomraning model for the set of benchmark problems described in Section 2. We assess the accuracy of the ensemble-averaged leakage at $x=L$, $\langle J_L\rangle$, computed using the Levermore-Pomraning model compared to the benchmark values using a relative error computed as

$$E_{\langle J_L\rangle}=\frac{\langle J_L\rangle_{LP}-\langle J_L\rangle_{benchmark}}{\langle J_L\rangle_{benchmark}}\ \ . \tag{16}$$

We assess the accuracy of the scalar flux distributions using a root-mean-squared (RMS) relative error computed as

$$E_{\langle\phi\rangle}=\sqrt{\frac{1}{N}\sum_{j=0}^{N-1}\left(\frac{\left\langle\phi_{LP}^j\right\rangle-\left\langle\phi_{benchmark}^j\right\rangle}{\left\langle\phi_{benchmark}^j\right\rangle}\right)^2}\ \ , \tag{17}$$

where $\langle\phi\rangle$ represents the ensemble-averaged total or material scalar flux distribution, $\langle\phi\left(x\right)\rangle$ or $\langle\phi_i\left(x\right)\rangle$, $i=0,1$, respectively, and the summation is over the $N=100$ spatial zones. The benchmark scalar flux results were computed using a discrete ordinates code with a linear discontinuous spatial discretization [6]. The Levermore-Pomraning results were computed using the simple corner balance spatial discretization [7] in which balance equations are written over half-zones ("corners"), and the unknowns are the half-zone-averaged ("corner-averaged") angular fluxes. The zone-averaged angular flux (and hence scalar flux) can be computed as an appropriate volume average of the half-zone quantities. We compare the Levermore-Pomraning zone-average

scalar flux values with the benchmark zone-average values computed as the algebraic average of the zone-edge values (consistent with the linear discontinous discretization).

The benchmark and Levermore-Pomraning values of the leakage $\langle J_L \rangle$ are shown in Tables II–IV along with the corresponding relative errors. The accuracy of the leakage computed by the Levermore-Pomraning model generally improves as the slab width decreases. The Levermore-Pomraning model accurately computes the leakage from the slab, to significantly less than 1%, for the $L = 0.1$ slabs. The largest errors for the $L = 1.0$ slab width are on the order of 1%. For the $L = 10.0$ slab width, the relative errors in the leakage computed by the Levermore-Pomraning model are typically a few percent, with the largest error approximately 10%.

Table II. Leakage $\langle J_L \rangle$ comparisons for case 1

Case	L	Benchmark	Levermore-Pomraning	Relative Error $E_{\langle J_L \rangle}$
0.1	a	0.48754	0.48755	2.05e-05
	b	0.46595	0.46578	-3.65e-04
	c	0.49250	0.49244	-1.22e-04
1.0	a	0.42520	0.42605	2.00e-03
	b	0.34760	0.34412	-1.00e-02
	c	0.44695	0.44494	-4.50e-03
10.0	a	0.15263	0.16575	8.60e-02
	b	0.07307	0.06934	-5.10e-02
	c	0.17484	0.17284	-1.14e-02
			RMS of $E_{\langle J_L \rangle}$	3.37e-02

The RMS relative errors for the total and material scalar flux distributions computed by the Levermore-Pomraning model are shown in Tables V–VII. As in the case of the leakage values, the accuracy of the Levermore-Pomraning model scalar flux distributions generally improves as the slab width decreases. The Levermore-Pomraning model scalar flux distribution errors are generally significantly less than 1% for the $L = 0.1$ slabs. The RMS relative errors for the $L = 1.0$ slabs are generally a few percent, with the maximum error being 27% for case 2a. The RMS relative errors for the $L = 10.0$ slabs are generally somewhat larger, with a maximum error of 62% again for case 2a.

Table III. Leakage $\langle J_L \rangle$ comparisons for case 2

Case	L	Benchmark	Levermore-Pomraning	Relative Error $E_{\langle J_L \rangle}$
0.1	a	0.48746	0.48746	0.00e+00
	b	0.47027	0.47013	-2.98e-04
	c	0.49246	0.49242	-8.12e-05
1.0	a	0.42543	0.42477	-1.55e-03
	b	0.43594	0.43487	-2.45e-03
	c	0.45494	0.45331	-3.58e-03
10.0	a	0.19073	0.19537	2.43e-02
	b	0.29302	0.26783	-8.60e-02
	c	0.31357	0.28361	-9.55e-02
			RMS of $E_{\langle J_L \rangle}$	4.36e-02

Table IV. Leakage $\langle J_L \rangle$ comparisons for case 3

Case	L	Benchmark	Levermore-Pomraning	Relative Error $E_{\langle J_L \rangle}$
0.1	a	0.49823	0.49823	0.00e+00
	b	0.43532	0.43533	2.30e-05
	c	0.49140	0.49140	0.00e+00
1.0	a	0.48812	0.48803	-1.84e-04
	b	0.29946	0.29926	-6.68e-04
	c	0.43577	0.43573	-9.18e-05
10.0	a	0.41133	0.40941	-4.67e-03
	b	0.12966	0.12577	-3.00e-02
	c	0.22563	0.21176	-6.15e-02
			RMS of $E_{\langle J_L \rangle}$	2.29e-02

We have plotted in Figs. 1–3 the total and material scalar flux distributions produced by the benchmark procedure and the Levermore-Pomraning model for cases 1b, 2a, and 3b and $L = 10$ as representative results. The statistical fluctuations in the case 1b $\langle \phi_1 (x) \rangle$ distribution derive from a small material probability $p_1 = 0.1$ resulting in a relatively small number of realizations contributing to the distribution. These statistical fluctuations were also observed in previous benchmark comparisons [4]. As is evident in Fig. 2, the case 2a material zero scalar flux is reasonably accurate (RMS relative error of 2.5%) while the material one scalar flux distribution

Table V. Scalar flux comparisons for case 1

			RMS Relative Error $E_{\langle\phi\rangle}$
L	Case	Quantity	Levermore-Pomraning
0.1	a	$\langle\phi\rangle$ $\langle\phi_0\rangle$ $\langle\phi_1\rangle$	7.71e-04 7.03e-04 2.63e-03
	b	$\langle\phi\rangle$ $\langle\phi_0\rangle$ $\langle\phi_1\rangle$	6.51e-04 5.87e-04 1.57e-03
	c	$\langle\phi\rangle$ $\langle\phi_0\rangle$ $\langle\phi_1\rangle$	8.48e-04 1.11e-03 8.25e-03
1.0	a	$\langle\phi\rangle$ $\langle\phi_0\rangle$ $\langle\phi_1\rangle$	2.00e-02 1.56e-02 8.48e-02
	b	$\langle\phi\rangle$ $\langle\phi_0\rangle$ $\langle\phi_1\rangle$	9.44e-03 1.01e-02 2.38e-02
	c	$\langle\phi\rangle$ $\langle\phi_0\rangle$ $\langle\phi_1\rangle$	2.07e-02 2.51e-02 5.71e-02
10.0	a	$\langle\phi\rangle$ $\langle\phi_0\rangle$ $\langle\phi_1\rangle$	5.00e-02 4.65e-02 1.08e-01
	b	$\langle\phi\rangle$ $\langle\phi_0\rangle$ $\langle\phi_1\rangle$	6.55e-02 6.74e-02 1.19e-02
	c	$\langle\phi\rangle$ $\langle\phi_0\rangle$ $\langle\phi_1\rangle$	1.39e-01 1.50e-01 4.26e-02
		RMS of $E_{\langle\phi\rangle}$	5.47e-02
		RMS of $E_{\langle\phi_0\rangle}$	5.80e-02
		RMS of $E_{\langle\phi_1\rangle}$	5.24e-02

exhibits large pointwise errors (RMS relative error of 62%). For this case, materials zero and one have mean material slab widths of one and ten, respectively. Material one is purely scattering and optically thick, conditions under which the Levermore-Pomraning model is known to be only approximate. Material zero is purely absorbing, and hence the Levermore-Pomraning model

Table VI. Scalar flux comparisons for case 2

			RMS Relative Error $E_{\langle\phi\rangle}$
L	Case	Quantity	Levermore-Pomraning
0.1	a	$\langle\phi\rangle$ $\langle\phi_0\rangle$ $\langle\phi_1\rangle$	5.16e-04 5.48e-04 9.64e-04
	b	$\langle\phi\rangle$ $\langle\phi_0\rangle$ $\langle\phi_1\rangle$	6.15e-04 5.59e-04 6.63e-04
	c	$\langle\phi\rangle$ $\langle\phi_0\rangle$ $\langle\phi_1\rangle$	5.61e-04 5.47e-04 9.86e-04
1.0	a	$\langle\phi\rangle$ $\langle\phi_0\rangle$ $\langle\phi_1\rangle$	3.41e-02 1.04e-02 2.73e-01
	b	$\langle\phi\rangle$ $\langle\phi_0\rangle$ $\langle\phi_1\rangle$	2.19e-03 1.91e-03 1.42e-02
	c	$\langle\phi\rangle$ $\langle\phi_0\rangle$ $\langle\phi_1\rangle$	4.46e-03 6.52e-03 4.23e-02
10.0	a	$\langle\phi\rangle$ $\langle\phi_0\rangle$ $\langle\phi_1\rangle$	1.77e-01 2.49e-02 6.20e-01
	b	$\langle\phi\rangle$ $\langle\phi_0\rangle$ $\langle\phi_1\rangle$	8.17e-02 8.25e-02 1.37e-01
	c	$\langle\phi\rangle$ $\langle\phi_0\rangle$ $\langle\phi_1\rangle$	1.34e-01 1.45e-01 3.14e-01
		RMS of $E_{\langle\phi\rangle}$	7.98e-02
		RMS of $E_{\langle\phi_0\rangle}$	5.63e-02
		RMS of $E_{\langle\phi_1\rangle}$	2.53e-01

should be generally more accurate.

Table VII. Scalar flux comparisons for case 3

			RMS Relative Error $E_{\langle\phi\rangle}$
L	Case	Quantity	Levermore-Pomraning
0.1	a	$\langle\phi\rangle$ $\langle\phi_0\rangle$ $\langle\phi_1\rangle$	1.02e-03 1.60e-03 2.93e-04
	b	$\langle\phi\rangle$ $\langle\phi_0\rangle$ $\langle\phi_1\rangle$	1.10e-03 1.55e-03 2.56e-04
	c	$\langle\phi\rangle$ $\langle\phi_0\rangle$ $\langle\phi_1\rangle$	1.03e-03 1.60e-03 3.09e-04
1.0	a	$\langle\phi\rangle$ $\langle\phi_0\rangle$ $\langle\phi_1\rangle$	3.31e-03 4.57e-03 1.33e-02
	b	$\langle\phi\rangle$ $\langle\phi_0\rangle$ $\langle\phi_1\rangle$	6.35e-04 1.00e-03 1.52e-03
	c	$\langle\phi\rangle$ $\langle\phi_0\rangle$ $\langle\phi_1\rangle$	1.60e-03 2.84e-03 1.09e-03
10.0	a	$\langle\phi\rangle$ $\langle\phi_0\rangle$ $\langle\phi_1\rangle$	2.82e-01 9.71e-02 4.32e-01
	b	$\langle\phi\rangle$ $\langle\phi_0\rangle$ $\langle\phi_1\rangle$	2.39e-02 2.49e-02 1.21e-02
	c	$\langle\phi\rangle$ $\langle\phi_0\rangle$ $\langle\phi_1\rangle$	9.74e-02 1.50e-01 6.33e-02
		RMS of $E_{\langle\phi\rangle}$	9.97e-02
		RMS of $E_{\langle\phi_0\rangle}$	6.01e-02
		RMS of $E_{\langle\phi_1\rangle}$	1.46e-01

5. CONCLUSIONS

We have investigated the accuracy of the Levermore-Pomraning model for particle transport through a binary stochastic medium using an interior source benchmark problem. As in previous

comparisons of the model for incident angular flux benchmark problems [3], the model accurately computes the leakage from optically thin slabs. The model is less accurate for more optically thick slabs but has a maximum relative error in the leakage of approximately 10% for the problems examined. The total and material scalar flux distributions exhibit similar trends, although the maximum root-mean-squared relative errors for the more optically thick slabs approach 65%.

Overall, we find that the Levermore-Pomraning model produces qualitatively and semi-quantitatively correct results for both the leakage values and the scalar flux distributions for this interior source benchmark problem. The leakage values are accurate to within approximately 10%, while the total and material scalar flux distributions can exhibit significantly larger pointwise and RMS relative errors. These findings are consistent with previous benchmark comparisons of leakage and scalar flux distributions for the incident angular flux benchmark problem [3, 4].

The benchmark and model comparisons and functionality described in this paper may serve as a foundation for investigating algorithms for the solution of eigenvalue problems in a binary stochastic medium. Benchmark results for eigenvalue problems with two-energy groups in planar geometry have previously been generated [12], but no model comparisons have been performed. Such benchmark and model comparisons could be useful for testing algorithms aimed at modelling pebble bed type reactors.

The appearance of the factor $|\mu|$ in the closure term of the Levermore-Pomraning equations has been conjectured as a source of inaccuracy of the model for slab geometry problems. This $|\mu|$ factor does not appear in the closure term in two and three dimensions. While it is difficult to generate realizations of Markovian statistics in multiple dimensions, it may be possible to perform a similar benchmark comparison of the Levermore-Pomraning model for different material statistics.

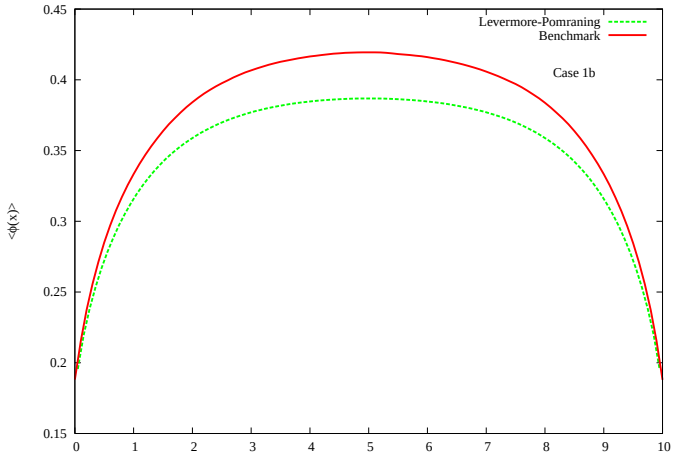

(a) $\langle \phi(x) \rangle$

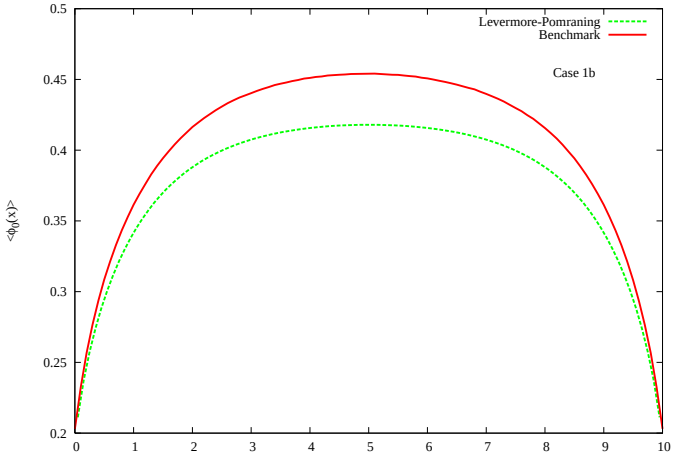

(b) $\langle \phi_0(x) \rangle$

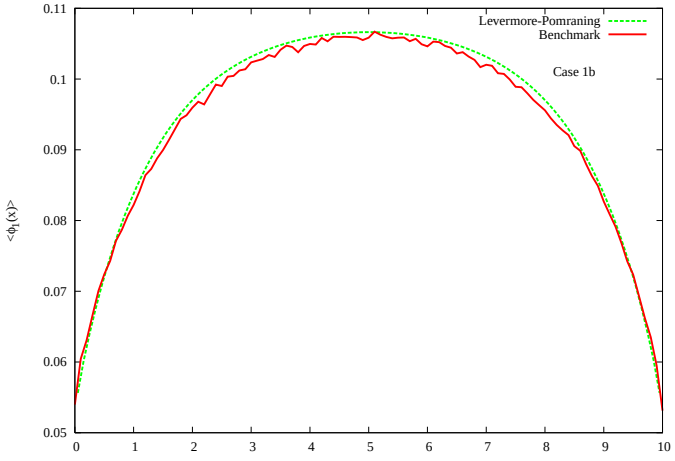

(c) $\langle \phi_1(x) \rangle$

Figure 1. Scalar flux distribution comparison for case 1b and L = 10

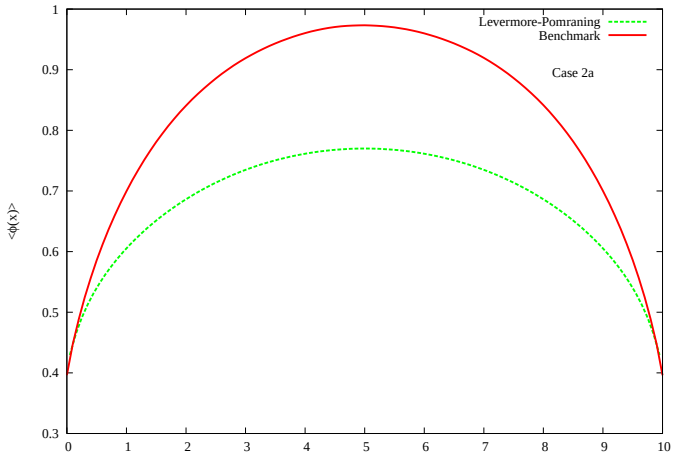

(a) $\langle \phi\,(x)\rangle$

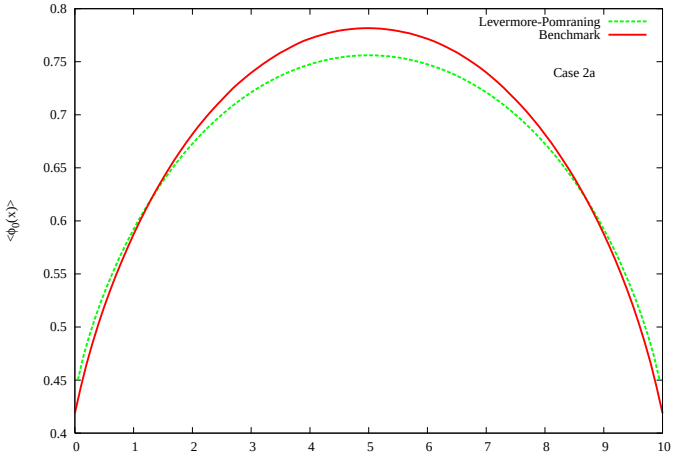

(b) $\langle \phi_0\,(x)\rangle$

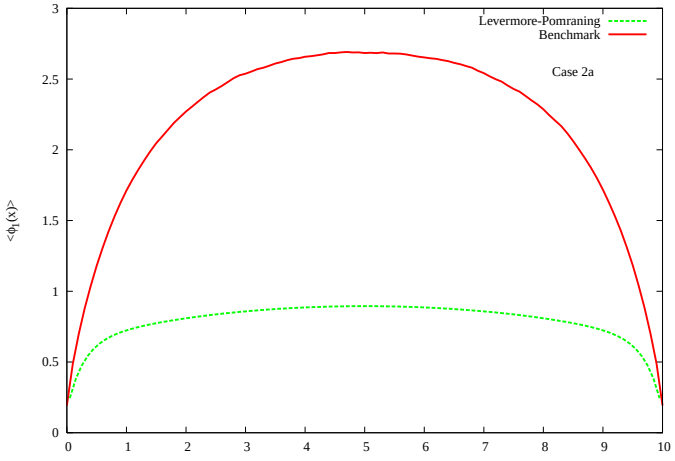

(c) $\langle \phi_1\,(x)\rangle$

Figure 2. Scalar flux distribution comparison for case 2a and L = 10

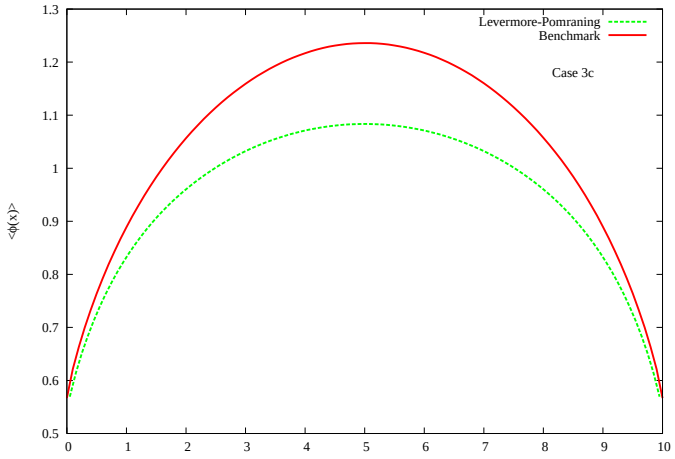

(a) $\langle \phi(x) \rangle$

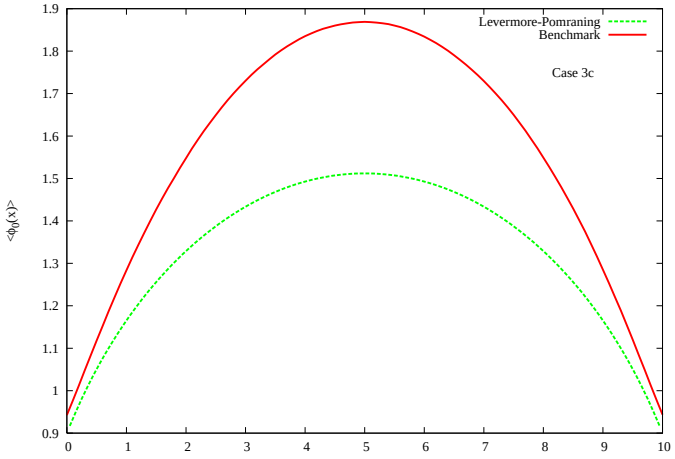

(b) $\langle \phi_0(x) \rangle$

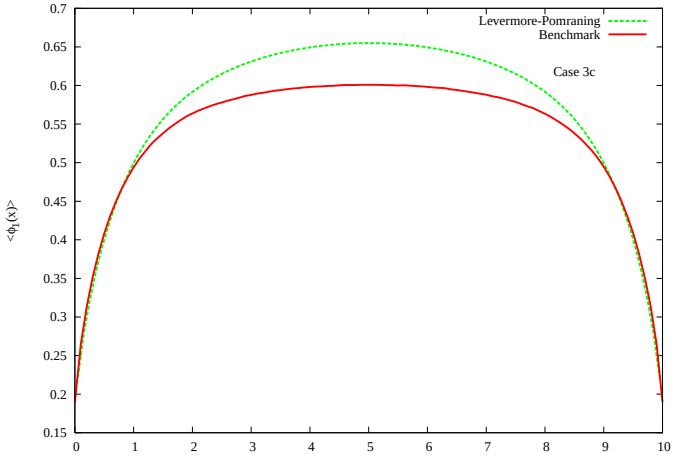

(c) $\langle \phi_1(x) \rangle$

Figure 3. Scalar flux distribution comparison for case 3c and L = 10

ACKNOWLEDGEMENTS

The work of the first author (P.S.B.) was performed under the auspices of the U.S. Department of Energy by Lawrence Livermore National Laboratory under Contract DE-AC52-07NA27344.

REFERENCES

[1] C. D. Levermore, G. C. Pomraning, D. L. Sanzo, and J. Wong, "Linear transport theory in a random medium," *J. Math. Phys.*, **27**, pp. 2526-2536 (1986).

[2] G. C. Pomraning, *Linear Kinetic Theory and Particle Transport in Stochastic Mixtures*, World Scientific Publishing Co. Pte. Ltd., River Edge, New Jersey USA (1991).

[3] M. L. Adams, E. W. Larsen, and G. C. Pomraning, "Benchmark Results for Particle Transport in a Binary Markov Statistical Medium," *J. Quant. Spectrosc. Radiat. Transfer*, **42**, pp. 253-266 (1989).

[4] O. Zuchuat, R. Sanchez, I. Zmijarevic, and F. Malvagi, "Transport in Renewal Statistical Media: Benchmarking and Comparison With Models," *J. Quant. Spectrosc. Radiat. Transfer*, **51**, pp. 689-722 (1994).

[5] R. Sanchez, "A Critique of the Modified Levermore-Pomraning Equations," *Ann. Nucl. Energy*, **35**, pp. 446-457 (2008).

[6] E. E. Lewis and W. F. Miller, *Computational Methods of Neutron Transport*, American Nuclear Society, Lagrange Park, Illinois, USA (1993).

[7] M. L. Adams, "Subcell Balance Methods for Radiative Transfer on Arbitrary Spatial Grids," *Trans. Theory Stat. Phys.*, **26** (1997).

[8] T. S. Palmer, "A Coupled Diffusion Synthetic Acceleration for Binary Stochastic Mixture Transport Iterations," *Nucl. Sci. Engr.*, **158**, pp. 40-48 (2008).

[9] P. Miller, "pyMPI - An Introduction to Parallel Python Using MPI ," Lawrence Livermore National Laboratory report UCRL-WEB-151052 (2002). See also http://pympi.sourceforge.net (2009).

[10] W. Gropp, E. Lusk, and A. Skjellum, *Using MPI: Portable Parallel Programming with the Message-Passing Interface*, The MIT Press, Cambridge, Massachusetts, USA (1999).

[11] O. Zuchuat, personal communication (2008).

[12] I. M. Davis and T. S. Palmer, "Two-Group k-Eigenvalue Benchmark Calculations for Planar Geometry Transport in a Binary Stochastic Medium," *Proceedings of the International Topical Meeting on Mathematics and Computation, Supercomputing, Reactor Physics and Nuclear and Biological Applications (M&C 2005)*, Palais des Papes, Avignon, France, September 12-15, 2005, on CD-ROM (2005).